NEOPLASIA
www.neoplasia.com

Volume 13 Number 2 February 2011 pp. 154–166 154

A Feedback Loop between Androgen Receptor and ERK Signaling in Estrogen Receptor–Negative Breast Cancer[1]

Kee Ming Chia*, Ji Liu*, Glenn D. Francis† and Ali Naderi*

*University of Queensland Diamantina Institute, Princess Alexandra Hospital, Brisbane, Queensland, Australia; †Pathology Queensland, Princess Alexandra Hospital, Brisbane, Queensland, Australia

Abstract

Estrogen receptor (ER)–negative breast cancer is heterogeneous, and the biology of this disease has remained poorly understood. Molecular apocrine is a subtype of ER-negative breast cancer that is characterized by the overexpression of steroid-response genes such as *AR* and a high rate of ErbB2 amplification. In this study, we have identified a positive feedback loop between the AR and extracellular signal–regulated kinase (ERK) signaling pathways in molecular apocrine breast cancer. In this process, AR regulates ERK phosphorylation and kinase activity. In addition, AR inhibition results in the down-regulation of ERK target proteins phospho-RSK1, phospho–Elk-1, and c-Fos using an *in vivo* molecular apocrine model. Furthermore, we show that AR-mediated induction of ERK requires ErbB2, and AR activity, in turn, regulates ErbB2 expression as an AR target gene. These findings suggest that ErbB2 is an upstream connector between the AR and ERK signaling pathways. Another feature of this feedback loop is an ERK-mediated regulation of AR. In this respect, the inhibition of ERK phosphorylation reduces AR expression and CREB1-mediated transcriptional regulation of AR acts as a downstream connector between the AR and ERK signaling pathways in molecular apocrine cells. Finally, we demonstrate that AR-positive staining is associated with the overexpression of ERK signaling targets phospho–Elk-1 and c-Fos in ER-negative breast tumors, which further supports a cross-regulation between the AR and ERK signaling pathways in molecular apocrine subtype. This study demonstrates an AR-ERK feedback loop in ER-negative breast cancer with significant biologic and therapeutic implications in this disease.

Neoplasia (2011) 13, 154–166

Introduction

Estrogen receptor–negative (ER–) breast cancer constitutes around 30% of all cases and commonly affects a younger patient population than ER+ disease [1]. In contrast to ER+ breast cancer, where the estrogen receptor signaling has a critical biologic and therapeutic role, ER– breast cancer is heterogeneous, and there is limited knowledge available regarding the pathophysiology of this disease.

Using expression microarray profiling, ER– breast cancer can be classified into molecular apocrine and basal subtypes [2]. Molecular apocrine subtype is characterized by a steroid-response gene signature that includes androgen receptor (AR) and a high frequency of ErbB2 overexpression [2–4]. Subsequent studies have demonstrated that AR is expressed in approximately 50% of ER– breast cancers and more than 50% of these cases also have ErbB2 overexpression [5–8]. Furthermore, it has recently been suggested that a loss of PTEN at early stages of tumorigenesis predisposes to the formation of breast tumors with molecular apocrine features [9].

The AR signaling pathway has a significant role in the proliferation and survival of molecular apocrine breast cancer cells [4,5,10]. Notably, there is a therapeutic value in the inhibition of AR using *in vitro* and *in vivo* models of molecular apocrine cells [4,5,10]. In this respect, there is currently an ongoing clinical trial evaluating the efficacy of AR inhibition in patients with AR+/ER– breast cancer (ClinicalTrials.gov identifier: NCT00468715). Moreover, we have identified a cross talk between the AR and ErbB2 signaling in molecular apocrine cells that modulates cell proliferation and expression of steroid-response genes

Address all correspondence to: Ali Naderi, Level 4, R Wing, Bldg 1, Princess Alexandra Hospital, Ipswich Rd, Brisbane, Queensland 4102, Australia. E-mail: a.naderi@uq.edu.au
[1]This study is funded by grants from the University of Queensland, the Princess Alexandra Hospital Cancer Collaborative Group, and Cancer Council Queensland.
Received 12 September 2010; Revised 14 October 2010; Accepted 18 October 2010

DOI 10.1593/neo.101324

[5]. In addition, a recent meta-analysis study has further confirmed this cross talk and demonstrated that there are interactions between the AR pathway, epidermal growth factor receptor trafficking signals, and ErbB2 in molecular apocrine breast cancer [11].

Although the mechanism of cross talk between AR and ErbB2 is not understood, we have found that extracellular signal–regulated kinase (ERK) phosphorylation is modulated in this process [5]. ERK is a critical downstream target of epidermal growth factor receptor–ErbB2 and activates signaling proteins such as 90-kDa ribosomal S6 kinases (RSK) and transcription factor Elk-1 that are versatile mediators of ERK signal transduction [12–14]. Moreover, we have recently demonstrated that the combination of AR inhibition and persistent ERK phosphorylation using flutamide and a Cdc25A phosphatase inhibitor PM-20, respectively result in a synergistic reduction of cell growth in molecular apocrine cells [10]. Importantly, this effect is associated with a synergistic reduction of RSK and Elk-1 phosphorylation and down-regulation of steroid-response genes [10]. Together, these findings raise the possibility of an interaction between the AR and ERK signaling pathways in molecular apocrine breast cancer. Interestingly, a cross talk between AR and ERK has been reported in prostate cancer and contributes to the progression of this disease [15]. Study of a possible interaction between the AR and ERK signaling pathways and identification of a molecular mechanism for this process would significantly advance our understanding of molecular apocrine breast cancer and potentially lead to the development of novel targeted therapies in this disease.

In this study, we investigate a cross-regulation between the AR and ERK signaling using *in vitro* and *in vivo* models. Our results suggest a feedback loop between the AR and ERK signaling pathways involving ErbB2 and CREB1 in molecular apocrine breast cancer.

Materials and Methods

Cell Culture and Treatments

Breast cancer cell lines MDA-MB-453, HCC-1954, and MCF-7 were obtained from American Type Culture Collection (Manassas, VA). All the culture media were obtained from Invitrogen (Melbourne, Australia). MDA-MB-453 and HCC-1954 cell lines were cultured in L15 media, 10% FBS and RPMI 1640 media, 10% FBS, respectively. MCF-7 cell line was cultured in Dulbecco modified Eagle medium/F12 media, 10% FBS. The following treatments were applied for the cell culture experiments: 1) AR inhibitor, flutamide (Sigma-Aldrich, Sydney, Australia) at 25 to 80 μM concentrations; 2) 5α-androstan-17β-ol-3-one (dihydrotestosterone [DHT]; Sigma-Aldrich) at 100 nM concentration [16]; 3) MEK inhibitor CI-1040 (PD184352; Selleck Chemicals, Houston, TX) at 2 to 10 μM concentrations; and 4) ErbB2 inhibitor, AG825 (Calbiochem, Melbourne, Australia) at 10 μM concentration. Treatments with the inhibitors were performed in medium containing FBS. DHT treatment was carried out in phenol red–free Dulbecco modified Eagle medium (Invitrogen) with 10% charcoal/dextran–treated serum (HyClone, Melbourne, Australia), and cell lines were cultured in this medium for 48 hours before DHT treatment.

Western Blot Analysis

Rabbit monoclonal ERK1/2 antibody, rabbit monoclonal phospho-ERK1/2 (Thr202/Tyr204) antibody, rabbit polyclonal AR antibody, and rabbit polyclonal ErbB2 antibody were obtained from Cell Signaling (Danvers, MA). Western blots were carried out at 1:1000 dilution of each primary antibody using 20 and 30 μg of cell lysates for the total and phospho-proteins, respectively. Protein concentrations from the cell isolates were measured using the BCA Protein Assay Kit (Thermo Scientific, Melbourne, Australia). Rabbit polyclonal α-tubulin antibody (Abcam, Cambridge, UK) was used as the loading control. Analysis of band densities was performed using Bio-Profil Densitometer Software (Vilber Lourmat, Eberhardzell, Germany). All fold changes in band densities were measured relative to the control groups. Western blots were done in two biologic replicates, and the average fold change was shown for each set of experiments.

AR Knockdown in Cell Lines

AR knockdown (KD) was carried out using the following small interfering (siRNA) oligos (duplex; Sigma-Genosys, Sydney, Australia): D1 5′CCAUCUUUCUGAAUGUCCU and D2 5′AGGACAUUCAGAAAGAUGG as described before [17]. Transfection of siRNA oligos using Lipofectamine RNAiMAX (Invitrogen) was carried out by reverse transfection method as instructed by the manufacturer. The final siRNA duplex concentration was 10 nM for the knockdown experiments. Cells transfected with siRNA Universal Negative Control no. 1 (Sigma-Genosys) were used as controls. In all experiments, the effects of AR-KD were assessed 72 hours after the siRNA transfections. All siRNA silencing experiments were performed in four replicates.

Real-time Polymerase Chain Reaction Analysis

Total RNA extraction was performed as described before [18]. Real-time polymerase chain reaction (RT-PCR) to assess the expression level of AR (assay ID, Hs00907244_m1) was carried out using TaqMan Gene Expression Assays (Applied Biosystems, Melbourne, Australia) as instructed by the manufacturer. Housekeeping genes *HPRT1* and *RPLP0* (Applied Biosystems) were used as controls. Relative gene expression = gene expression in the treated group/average gene expression in the control group. All experiments were performed in four biologic replicates.

ERK Kinase Assay

ERK kinase assay was carried out using MAP Kinase/ERK Immunoprecipitation Kinase Assay Kit (Millipore, Sydney, Australia) following the manufacturer's instructions. HCC-1954 and MDA-MB-453 cells were grown in full medium to 60% confluence in 150-mm tissue culture dishes. Next, DHT treatment was carried out for 3 and 12 hours in MDA-MB-453 and HCC-1954 lines, respectively. Immunoprecipitation was carried out using anti–MAP kinase–ERK1/2, agarose conjugate (Millipore), and immunoblot analysis was performed with 1 μg/ml of anti–phospho myelin basic protein as instructed by the manufacturer (Millipore). Vehicle-only–treated cells were used as a control.

Luciferase Reporter Assays

Full-length complementary DNA (cDNA) clones for CREB1 and c-Fos were obtained from Open Biosystems (Thermo Scientific). The clones were validated by restriction digestion/sequencing and then subcloned in a pcDNA3.1 vector (Invitrogen) to generate expression constructs. Full-length cDNA clone for Elk-1 in a pReciever expression vector was obtained from GeneCopoeia (Rockville, MD). Furthermore, the sequence of the 1.5-kb promoter region of AR was obtained using the Ensembl Genome Browser and PCR-generated using the following

primers: forward GCGCGGTACCCACAATGCCACGAGGCCCGA and reverse GCGCGAGCTCACTTGCGGGAGCAACCACGC. Subsequently, AR promoter was cloned in a pGL3 luciferase reporter vector (Promega, Sydney, Australia) and validated by restriction digestion/sequencing.

To carry out the reporter assays, MCF-7 cells were cotransfected with the AR reporter vector and each of the transcription factors using ExGen 500 reagent (Fermentas Life Sciences, St Leon-Rot, Germany). The *Renilla* pRL-TK vector (Promega) was used as an internal control reporter. Cotransfection with AR reporter vector and an empty pcDNA vector was used as a control. Forty-eight hours after the transfections, reporter activities were measured using Dual-Glo Luciferase Assay System (Promega) in an Orion II Microplate Luminometer (Berthold Detection Systems, Pforzheim, Germany). The response ratios for transcription factors and control were measured relative to the internal control reporter (relative response ratio). All reporter assays were carried out in four biologic replicates.

Bioinformatics Analysis

The sequence of the 1.5-kb promoter regions of ErbB2 and AR were obtained using the Ensembl Genome Browser (http://www.ensembl.org/index.html). Identification of putative transcription factor binding sites in these promoter regions was carried out using PATCH public 1.0 software (http://www.gene-regulation.com/cgi-bin/pub/programs/patch/bin/patch.cgi) and TRANSFAC 6.0 database (http://www.gene-regulation.com/cgi-bin/pub/databases/transpath/search.cgi). Data were then examined for the number and location of AR putative binding sites on ErbB2 promoter and that of CREB1, c-Fos, and Elk-1 transcription factors on AR promoter.

Chromatin Immunoprecipitation Assays

Chromatin immunoprecipitation (ChIP) assays were performed in MDA-MB-453 cell line using ChIP Assay Kit (USB Corporation, Cleveland, OH) as instructed by the manufacturer [19]. ChIP-grade rabbit monoclonal CREB1 (ChIPAb+ CREB Kit; Millipore) and rabbit polyclonal AR (Millipore) antibodies were applied for these assays at 1:100 dilutions. Two sets of primers for ErbB2 promoter and three sets of primers for AR promoter were used for the end point RT-PCR amplification using SYBR green method (Applied Biosystems). ErbB2 promoter primers included the following: Primer set 1, forward primer GCGCGAAGAGAGGGAGAAAGTGAA (start −345) and reverse primer CCAACAAGTCTGGGAGTGGCAACT (start −291); and Primer set 2, forward primer GGATGCAAGCTCCCCAGGAAAGTT (start −549) and reverse primer CCCTAAATGCAGAGGCTGGTGACT (start −421). AR promoter primers included the following: Primer set 1, forward primer TGCCCTTTCCTCTTCGGTGAAGT (start −382) and reverse primer ACCAGGCACTTTCCTTGCTTCCT (start −312); Primer set 2, forward primer GGAAAGCAGGAGCTATTCAGGAAGCA (start −842) and reverse primer CCTGCCTAGTGGCTTTGGAGAAACAA (start −733); and Primer set 3, forward primer GCAAGCGGCTGCATACAAAGCAAA (start −1375) and reverse primer TGCCATGTACACATAGGCGCTCAAT (start −1304). Amplification of input chromatin before immunoprecipitation at a dilution of 1:50 was used as a positive control. ChIP using negative control supernatant (ChIPAb+ CREB Kit; Millipore) and nonspecific antibody (rabbit IgG) served as negative controls for AR and ErbB2 promoter ChIP assays, respectively. The assays were carried out in three replicates, and copy number changes were calculated as $-\text{Log}_2$ value for each experimental set.

Tumor Xenograft Studies

Animal ethics approval was obtained for the project, and mice were maintained in accordance with the Institutional Animal Care guidelines. Six-week-old female nonobese diabetic/severe combined immunodeficient mice were purchased from Animal Resource Center (WA, Australia). The method for generating the tumors in mice was performed as previously published [10,20]. A total of 5×10^6 MDA-MB-453 cells were injected into the flank of each mouse to generate the xenograft tumors [10]. Treatments were initiated 7 days after the cell injections. A total of 16 mice were studied in the following groups (four mice for each treatment or control group):

A) Flutamide experiments: 1) treatment with 25 mg/60-day slow-release flutamide pellets (Innovative Research of America, Sarasota, FL) and 2) control group with placebo pellets (Innovative Research of America). The pellets were implanted subcutaneously through a 1-cm incision on the flank of anesthetized mice.
B) MEK inhibitor experiments: 1) treatment with daily oral gavage of MEK inhibitor PD0325901 (Selleck Chemicals) at 15 mg/kg per day as described before [21]. PD0325901 was prepared at a stock concentration of 50 mg/ml in DMSO (Sigma-Aldrich) and made up to the daily working concentration in 0.05% methylcellulose/0.02% Tween-80 (Sigma-Aldrich). 2) Control group with daily gavage of an equal volume of DMSO to that of the treatment group in the same carrier solution.

Xenograft tumors were harvested 28 days after the start of treatment in each group. The harvested tumors were fixed in formalin and embedded in paraffin for immunohistochemistry (IHC) staining.

Immunohistochemistry

IHC staining was performed using EnVision+ System-HRP (AEC; DakoCytomation, Botany, Australia) following the manufacturer's instruction. Antigen retrieval was carried out using Target Retrieval Solution (DakoCytomation). The following primary antibodies were obtained from Abcam: rabbit polyclonal phospho–Elk-1 (S383), rabbit monoclonal phospho-RSK1 (T359 + S363), rabbit polyclonal c-Fos, and rabbit polyclonal AR. Primary antibody incubations were carried out at 1:50 dilution for phospho–Elk-1 and at 1:100 dilutions for the other antibodies. Slides were counterstained with hematoxylin (Sigma-Aldrich) and mounted using Glycergel Mounting Medium (DakoCytomation). For IHC scoring, slides were examined using a light microscope (Nikon Instruments, Inc, Tokyo, Japan). A total of 1000 cells per slide were counted at 60× magnification to assess the percentage of cells showing positive staining for each antibody. Scoring was carried out separately by two investigators, and the average scores were used for the final analysis.

Primary Breast Tumors

The institutional research ethics committee approved this study and informed consent was obtained from each patient for the use of tissue samples. A total of 24 paraffin-embedded ER– breast tumor samples were obtained from the Princess Alexandra Hospital tissue bank. IHC staining for AR, phospho–Elk-1, and c-Fos was carried out as described above. For downstream analysis, tumors were classified into two groups based on their AR staining pattern: 1) AR+ group with

20% of cells or more showing positive AR staining and 2) AR– group with less than 20% of cells stained for AR.

Statistical Analysis

Biostatistical analysis was done using SPSS version 17.0 (SPSS, Inc, Chicago, IL). Mann-Whitney *U* test was applied for the comparison of nonparametric data.

Results

AR Regulates the Phosphorylation of ERK

To investigate a possible AR regulation of ERK signaling, we first examined the effect of AR activation using DHT on the phosphorylation of ERK in molecular apocrine cells. MDA-MB-453 and HCC-1954 cell lines were treated with 100 nM of DHT at various time points, and the expression of total and phospho-ERK proteins was assessed using Western blot analysis. In MDA-MB-453 cells, we observed a rapid induction of phospho-ERK after DHT treatment, which lasted for 1 hour with a peak phospho-ERK/total-ERK ratio of 1.6-fold at 30 minutes compared with the untreated control (Figure 1*A*). Furthermore, in HCC-1954 cells, there was an induction of phospho-ERK at 30 minutes, which persisted for 12 hours after DHT treatment with a peak phospho-ERK/total-ERK ratio of 3.8-fold at 12 hours compared with the untreated control (Figure 1*B*). Moreover, there was no significant change in the amount of total-ERK after DHT treatments in these cell lines (Figure 1, *A* and *B*).

We next investigated the effect of AR inhibition using flutamide on ERK phosphorylation in MDA-MB-453 and HCC-1954 cell lines. Flutamide treatments were carried out for 48 hours before harvesting cell lysates for Western blot analysis. In addition, we examined a possible synergy between flutamide and MEK inhibitor CI-1040 in the reduction of ERK phosphorylation in these cell lines. CI-1040 treatments were carried out for 24 hours before harvesting cell lysates, and we tested the effect of various concentrations of CI-1040 on the phosphorylation of ERK. We observed that CI-1040 at 10-μM concentration almost completely inhibited ERK phosphorylation in both cell lines (Figure 1*C*). However, CI-1040 at 2 μM concentration resulted in a partial reduction of ERK phosphorylation in cell lines to around 0.21- to 0.26-fold compared with the controls (Figure 1, *D* and *E*).

Notably, in MDA-MB-453 cells, flutamide at 40 μM completely inhibited ERK phosphorylation, and the addition of flutamide at 25-μM concentration to CI-1040 at 2 μM resulted in a synergistic inhibition of ERK phosphorylation to undetectable levels (Figure 1, *D* and *E*). Moreover, a similar pattern of response was observed in the HCC-1954 cell line, in which flutamide at 60- and 80-μM concentrations resulted in a dose-dependent reduction of ERK phosphorylation to 0.58- and 0.29-fold compared with the controls (Figure 1*F*). Furthermore, in HCC-1954 cells, the addition of flutamide at 40-μM concentration to CI-1040 at 2 μM resulted in a synergistic inhibition of ERK phosphorylation to undetectable levels (Figure 1*D*). As observed with DHT experiments, we did not find any changes in the total ERK levels after flutamide treatment in molecular apocrine cells (Figure 1, *D*–*F*).

We further studied the effect of AR down-regulation on the phosphorylation of ERK using RNA interference. AR-KD was carried out using a siRNA duplex as described in the Materials and Methods section, and the efficiency of knockdown was assessed by RT-PCR and Western blot analysis. We observed an approximately 85% reduction of AR transcript and protein levels after AR-KD (Figure 2, *A* and *B*). It is notable that MDA-MB-453 cells showed a markedly higher baseline level of AR compared with HCC-1954 cells (Figure 2*B*). Furthermore, AR down-regulation resulted in the reduction of phospho-ERK/total-ERK ratio to 0.57-fold in MDA-MB-453 and to 0.9-fold in HCC-1954 cells (Figure 2*C*).

These findings suggest that AR activity is both necessary and sufficient for the phosphorylation of ERK in molecular apocrine cells. In addition, MDA-MB-453 cells show a higher degree of sensitivity to the effect of AR inhibition and knockdown in reducing ERK phosphorylation compared with HCC-1954 cells.

AR Induces ERK Kinase Activity

Because AR activation induces the phosphorylation of ERK, we next asked whether a similar effect can be observed for ERK kinase activity. MDA-MB-453 and HCC-1954 cell lines were treated with DHT at 100 nM concentration for 3 and 12 hours, respectively, and ERK activity was measured using immunoprecipitation kinase assay as described in the Materials and Methods section. We observed a low baseline ERK kinase activity in these cell lines (Figure 2*D*). Importantly, in both cell lines, there was a marked induction of ERK activity by three-fold compared with the controls after DHT treatment (Figure 2*D*). These findings suggest that AR activates ERK kinase in molecular apocrine cells.

ErbB2 Is Required for AR-Induced ERK Phosphorylation

It is known that ErbB2 has a critical role in the activation of ERK signaling [22]. In addition, we have previously shown a functional cross talk between the AR and ErbB2 pathways in molecular apocrine cells [5]. Therefore, we next investigated a possible role for ErbB2 in AR-mediated induction of ERK. MDA-MB-453 and HCC-1954 cell lines were treated with a selective ErbB2 inhibitor, AG825, at 10 μM for 24 hours before DHT treatment. DHT treatments were carried out for 1 hour and 12 hours in MDA-MB-453 and HCC-1954, respectively, corresponding to the peak DHT response in each cell line as shown before (Figure 1, *A* and *B*). Cell lines treated with AG825 alone were used as controls, and the expression of total and phospho-ERK proteins was assessed using Western blot analysis. It is notable that we did not observe any change in the level of ERK phosphorylation after DHT treatment in AG825-pretreated cell lines (Figure 3*A*). This finding suggests that ErbB2 activity is required for AR-mediated induction of ERK phosphorylation in molecular apocrine cells.

ErbB2 Is a Transcriptional Target of AR

Because ErbB2 activity is necessary for AR induction of ERK, we next examined a possible AR regulation of ErbB2 in molecular apocrine cells. In this respect, we first assessed the effect of AR activation using DHT on ErbB2 expression. MDA-MB-453 and HCC-1954 cell lines were treated with DHT for 1 hour and 12 hours, respectively, and the expression of ErbB2 was assessed using Western blot analysis. We observed that there was an increase in ErbB2 expression by 2.8- and 1.8-fold in MDA-MB-453 and HCC-1954 cells, respectively, after DHT treatment compared with the untreated controls (Figure 3*B*).

We next studied the effect of AR inhibition using flutamide on ErbB2 expression. MDA-MB-453 and HCC-1954 cell lines were treated with flutamide for 48 hours at 40- and 80-μM concentrations, respectively. There was a marked reduction of ErbB2 protein level to 0.2-fold in MDA-MB-453 and to 0.55-fold in HCC-1954 after flutamide treatments compared with the untreated controls (Figure 3*C*).

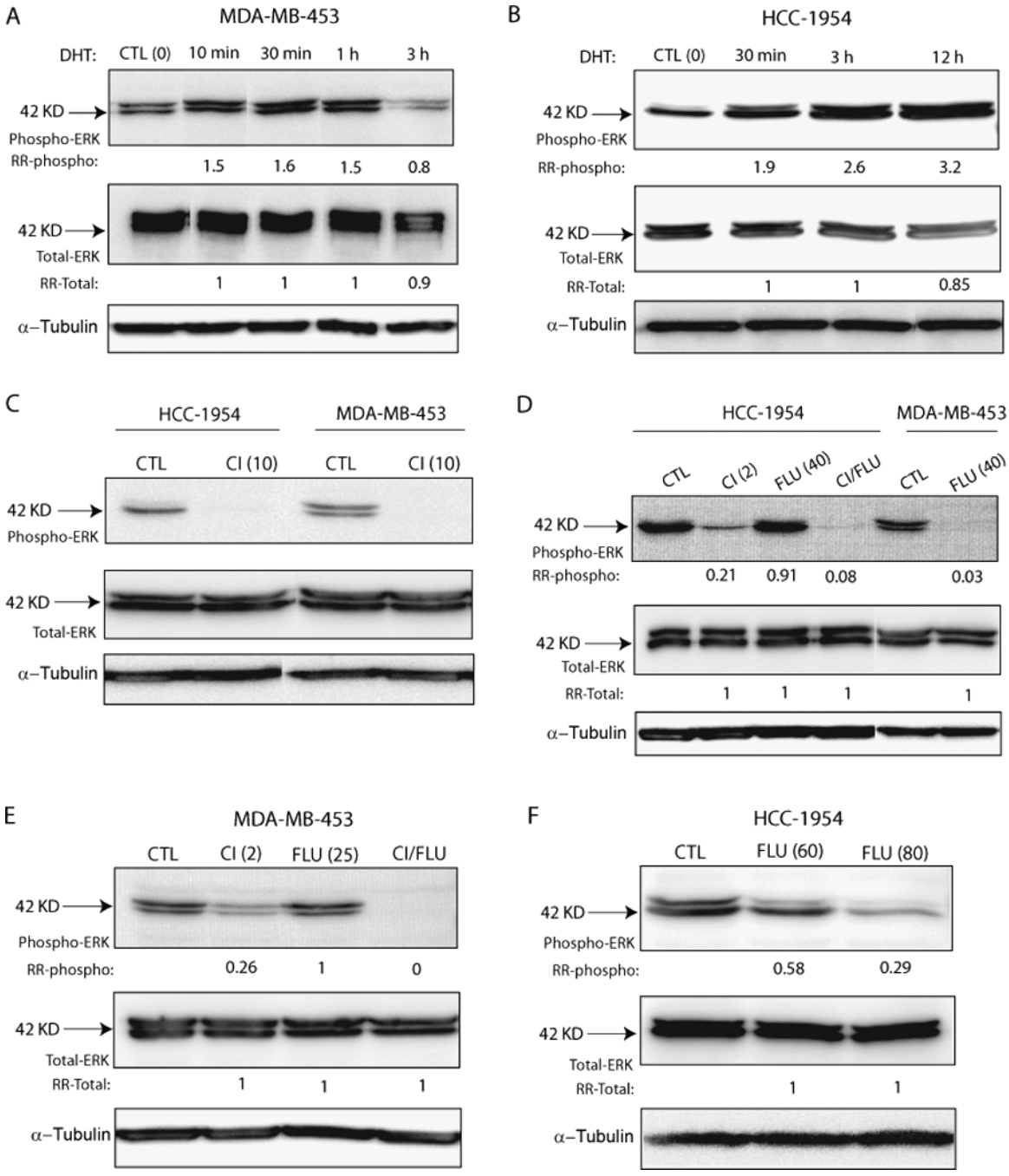

Figure 1. AR regulation of ERK phosphorylation. (A) Western blot analysis to measure the phosphorylated and total ERK levels in MDA-MB-453 cells after treatment with 100 nM of DHT at various time points. Fold changes (RR) in band densities were measured relative to the untreated control (CTL) and RR for phospho-ERK and total ERK were shown for each condition. (B) Western blot analysis to measure the phosphorylated and total ERK levels in HCC-1954 cells after treatment with DHT as described in (A). (C) Western blot analysis to measure the phosphorylated and total ERK levels in MDA-MB-453 and HCC-1954 cell lines after treatment with CI-1040 (CI) at 10-μM concentration. (D) Western blot analysis to measure the phosphorylated and total ERK levels in MDA-MB-453 and HCC-1954 cells after flutamide (FLU) and CI-1040 (CI) treatments. CI-1040 and flutamide treatments were carried out at 2- and 40-μM concentrations, respectively. (E) Western blot analysis to measure the phosphorylated and total ERK levels in MDA-MB-453 cells. CI-1040 (CI) and flutamide (FLU) treatments were carried out at 2- and 25-μM concentrations, respectively. (F) Western blot analysis to measure the phosphorylated and total ERK levels in HCC-1954 cells. Flutamide treatments were performed at 60- and 80-μM concentrations.

Furthermore, we assessed the effect of AR-KD on ErbB2 protein level and found that ErbB2 level was reduced to 0.33-fold in MDA-MB-453 and to 0.9-fold in HCC-1954 cells after AR-KD compared with control siRNA-transfected cell lines (Figure 3*D*). These findings suggest that AR activity is necessary and sufficient for ErbB2 expression.

To explain these observations, we first examined the 1.5-kb ErbB2 promoter region using bioinformatics programs and identified two AR putative binding sites at −556 and −577 bp. We next carried out ChIP assay to test AR binding to the ErbB2 promoter. Two sets of primers for ErbB2 promoter were used for the end point RT-PCR amplification

as described in the Materials and Methods section. Amplification of input chromatin at a dilution of 1:50 served as a positive control (Input) and ChIP using nonspecific antibody (rabbit IgG) as a negative control. Copy number changes were calculated as $-\text{Log}_2$ value for each experimental set (Figure 3*E*). Importantly, we observed enrichment for ErbB2 promoter region with AR antibody using each of the two primer sets ($P < .01$; Figure 3*E*). These findings demonstrate that AR binds to the ErbB2 promoter, and ErbB2 is an AR target gene.

ERK Regulates AR Expression

We have previously reported a synergistic down-regulation of steroid-response genes after the combined administration of Cdc25A phosphatase inhibitor PM-20 and flutamide that was accompanied with the down-regulation of ERK target proteins in molecular apocrine cells [10]. Therefore, we next explored the possibility of an ERK-mediated regulation of AR expression as an additional mechanism of interaction between these two pathways. To study this effect, MDA-MB-453 and HCC-1954 cell lines were treated with CI-1040 at 10-μM concentration for 24 hours, and vehicle (DMSO)-treated cells were used as controls. We then assessed AR expression using RT-PCR and observed a significant reduction of AR transcript level after MEK inhibition to 0.2- and 0.6-fold in MDA-MB-453 and HCC-1954 cells, respectively, compared with the controls ($P < .01$; Figure 4*A*). These findings suggest that ERK signaling regulates AR expression in molecular apocrine cells.

To explain the underlying mechanism for our findings, we investigated the effects of well-characterized ERK signaling transcription factors CREB1, Elk-1, and c-Fos on AR transcription [23–27]. Examination of the 1.5-kb AR promoter region identified several putative binding sites for these transcription factors (Figure 4*B*). We subsequently used luciferase reporter assays to examine the effects of these predicted transcription factors on the regulation of AR promoter. Because of a high degree of transfectability, MCF-7 cells were used for the reporter assay experiments [19]. MCF-7 cells were cotransfected with the AR reporter vector and each of the CREB1, Elk-1, and c-Fos expression constructs. Cotransfection with the AR reporter vector and an empty pcDNA vector was used as a control. Forty-eight hours after the transfections, reporter activities were measured, and relative response ratios were calculated as

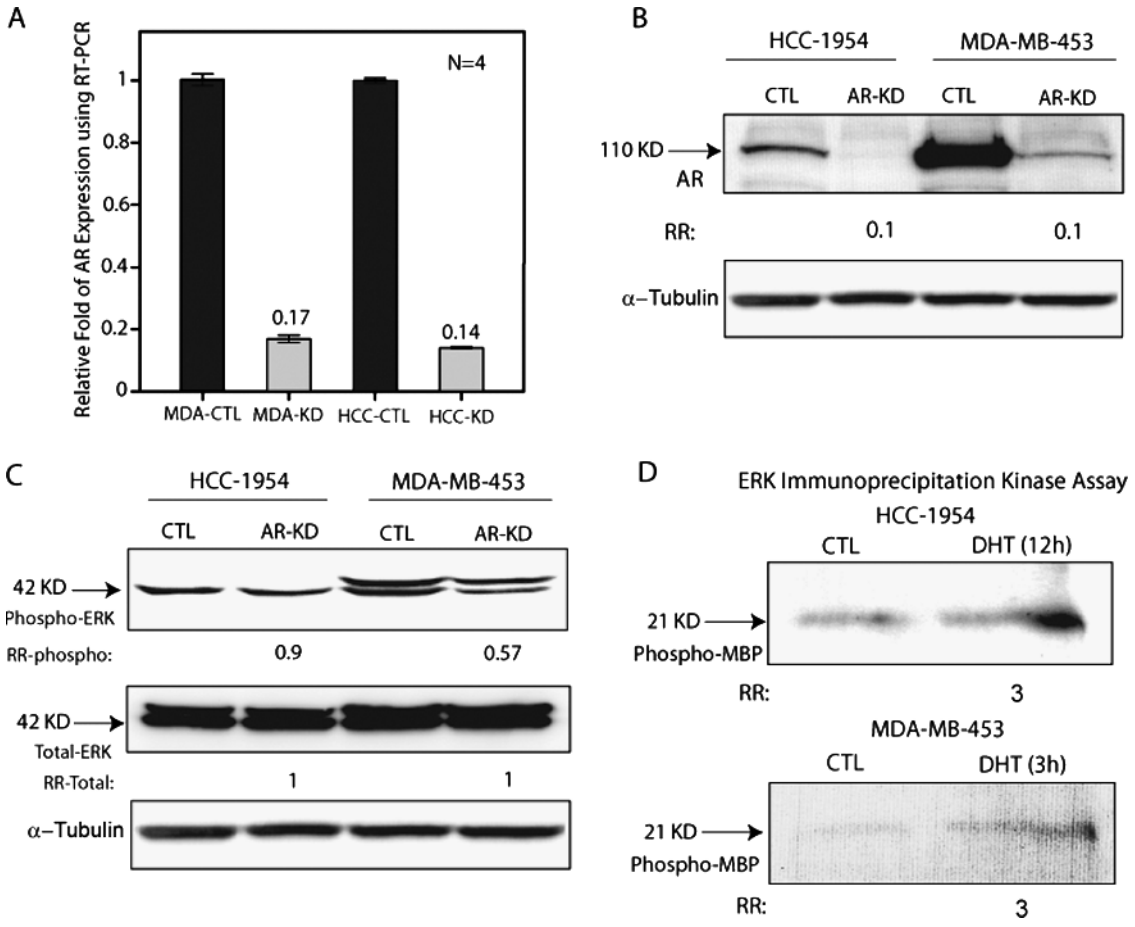

Figure 2. AR knockdown effect on ERK phosphorylation and DHT induction of ERK kinase activity. (A) RT-PCR to demonstrate AR knockdown (KD) efficiencies after AR-siRNA transfections in MDA-MB-453 (MDA) and HCC-1954 (HCC) cells. AR expression after knockdown was assessed relative to nontargeting siRNA control (CTL), and fold change is shown for each cell line. Error bars, ±2 SEMs. (B) Western blot analysis to show AR protein expression after AR-KD in MDA-MB-453 and HCC-1954 cells. Fold changes (RR) in band densities were measured relative to the control. (C) Western blot analysis to measure the phosphorylated and total ERK levels in MDA-MB-453 and HCC-1954 cell lines after AR-KD. (D) ERK kinase activity. ERK kinase assay was carried out using immunoprecipitation kinase assay. MDA-MB-453 and HCC-1954 cells were treated with DHT at 100-nM concentration for 3 and 12 hours, respectively. Fold changes (RR) in band densities after DHT treatment were measured relative to the control group.

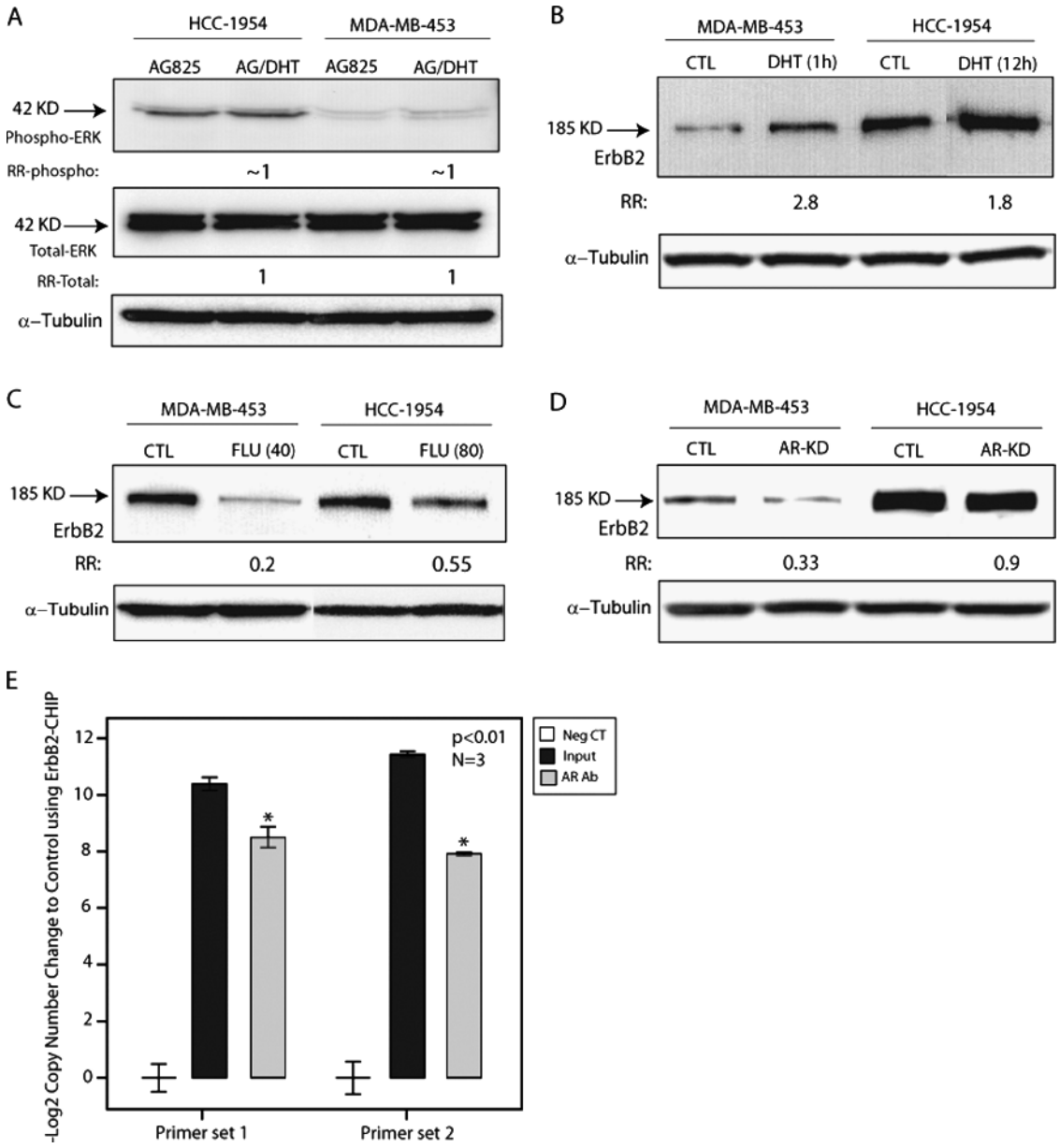

Figure 3. AR regulation of ErbB2 expression. (A) Western blot analysis to show the effect of ErbB2 inhibition on AR-induced ERK phosphorylation. AG825 (AG) treatment was carried out at 10 μM for 24 hours. DHT treatments were performed for 1 hour and 12 hours in MDA-MB-453 and HCC-1954 cells, respectively. Fold changes (RR) in band densities were measured relative to AG825-treated lines. (B) Western blot analysis to show the effect of DHT on ErbB2 protein level. DHT treatments were carried out as in (A). Fold changes (RR) in band densities were measured relative to the untreated controls. (C) Western blot analysis to show the effect of flutamide on ErbB2 protein level. Flutamide (FLU) treatments were carried out for 48 hours at 40- and 80-μM concentrations in MDA-MB-453 and HCC-1954 cell lines, respectively. (D) Western blot analysis to show the effect of AR knockdown (KD) on ErbB2 protein level in MDA-MB-453 and HCC-1954 lines. Fold changes (RR) in band densities were measured relative to nontargeting siRNA control. (E) ChIP assay with AR antibody. The results of end point RT-PCR amplification for ChIP assay are shown with two sets of primers for ErbB2 promoter. Input indicates input at a dilution of 1:50; Neg. CT, nonspecific antibody. The relative copy number changes to control are shown as $-\text{Log}_2$ values. *$P < .01$ is for AR Ab. *versus* Neg. CT. Error bars, ±2 SEMs.

described in the Materials and Methods section. We observed a marked increase in AR reporter activity with CREB1 by approximately 12-fold ($P < .01$; Figure 4*C*). In addition, Elk-1 and c-Fos did not activate the AR promoter (Figure 4*C*).

To test the binding of CREB1 to AR promoter we next carried out ChIP assay. Three sets of primers for AR promoter were used for the end point RT-PCR amplification. Amplification of input chromatin at a dilution of 1:50 and negative control supernatant were applied as positive and negative controls, respectively. Copy number changes were calculated as $-\text{Log}_2$ value for each experimental set (Figure 4*D*). Notably, we observed enrichment for the AR promoter region with CREB1 antibody using each of the three primer sets ($P < .01$; Figure 4*D*). These data demonstrate that AR is a CREB1 target gene.

AR Inhibition Results in the In Vivo *Down-regulation of ERK Target Proteins*

We further investigated the AR regulation of ERK signaling using an *in vivo* xenograft model of molecular apocrine breast cancer. Xenograft

tumors were generated using MDA-MB-453 cells as described in the Materials and Methods section. A total of four mice were treated with slow-release flutamide pellets for 28 days, and tumors were then harvested for IHC staining. Mice implanted with the placebo pellets were used as controls. We next carried out IHC staining for the ERK target proteins phospho–Elk-1, phospho-RSK1, and c-Fos in the harvested tumors. Subsequently, we determined the percentage of cells stained with each antibody and compared the results between flutamide-treated and placebo groups.

We observed that phospho–Elk-1, phospho-RSK1, and c-Fos expression were markedly lower in flutamide-treated group compared with the controls (Figure 5). In this respect, there was an approximately 20% staining for phospho–Elk-1 in flutamide-treated group compared with 60% in the control group ($P < .01$; Figure 5, *A*–*C*). Furthermore, a similar pattern was observed for phospho-RSK1 and c-Fos with an approximately three-fold lower staining for these proteins in flutamide-treated group compared with that in the controls ($P < .01$; Figure 5, *A* and *D*–*G*). These findings suggest that the inhibition of AR *in vivo* leads to the downregulation of ERK signaling proteins in molecular apocrine tumors.

ERK Inhibition Leads to an In Vivo *Reduction of AR Expression*

We subsequently evaluated the *in vivo* effect of ERK signaling inhibition on the expression of AR. Xenograft tumors were generated using MDA-MB-453 cells, and a total of four mice were treated with daily oral gavage of MEK inhibitor PD0325901 at 15 mg/kg per day for 28 days. Mice given daily gavage of an equal volume of DMSO/carrier solution to that of treatment group were used as controls. Xenograft tumors were harvested at the end of treatment period and stained

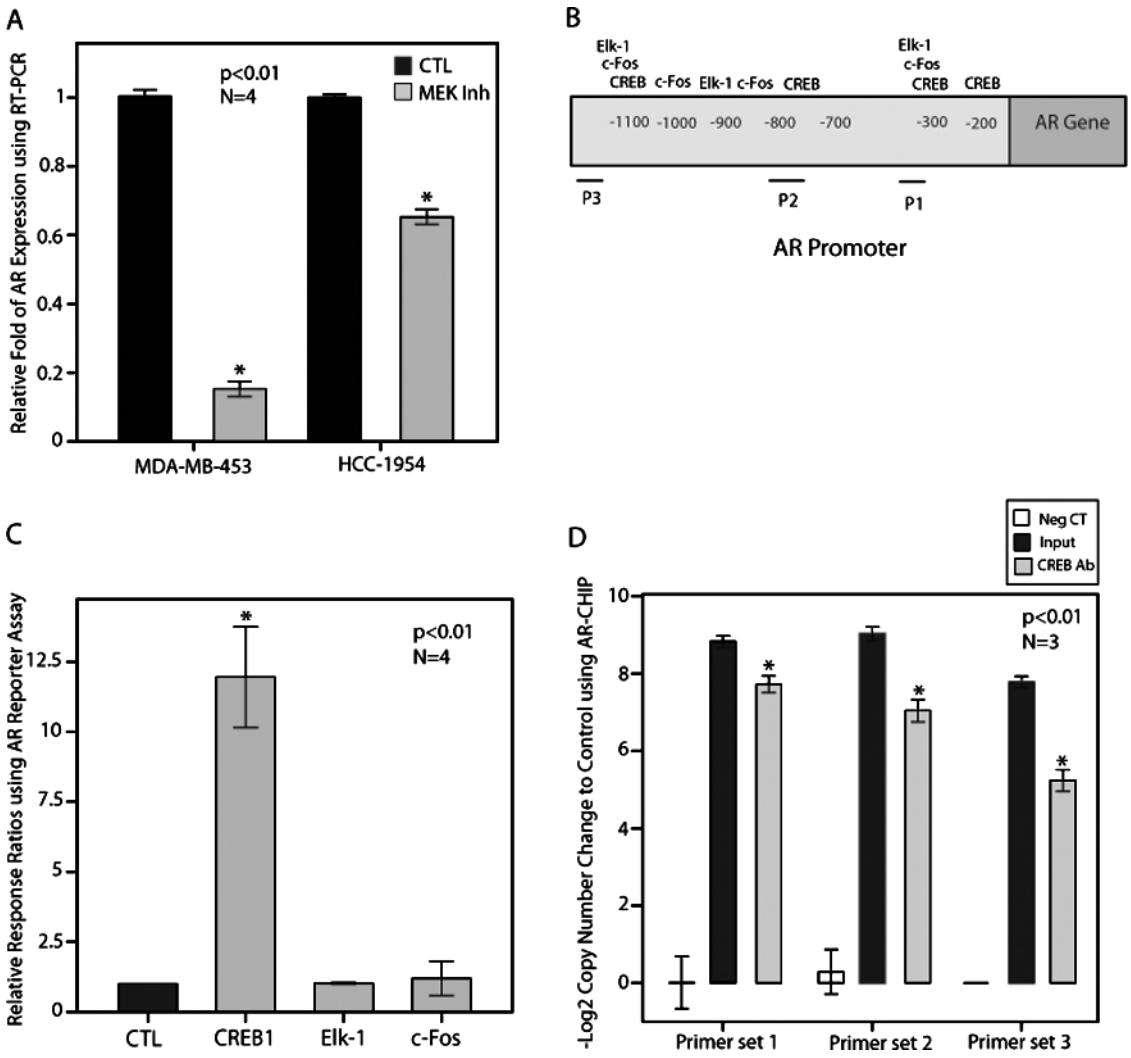

Figure 4. ERK regulation of AR expression. (A) Relative expression of AR using RT-PCR in MDA-MB-453 and HCC-1954 cell lines after treatment with CI-1040 (MEK Inh) at 10-μM concentration for 24 hours. Expression is relative to that of vehicle-treated cells (CTL). *$P < .01$ is for CI-1040 *versus* control. Error bars, ±2 SEMs. (B) Putative transcription factor binding sites for CREB1, Elk-1, and c-Fos in the 1.5-kb promoter region of AR. P1 (primer set 1), P2 (primer set 2), and P3 (primer set 3) are regions of amplification for ChIP assays. (C) Luciferase reporter assay. The transcriptional activation of AR promoter by CREB1, Elk-1, and c-Fos expression constructs was assessed using Dual-Luciferase Assays in MCF-7 cells, and relative response ratios are reported. Cotransfection with the AR reporter vector and an empty pcDNA vector was used as a control. *Compared with the control group. Error bars, ±2 SEMs. (D) ChIP assay with CREB1 antibody. The results of end point RT-PCR amplification for ChIP assay are demonstrated with three sets of primers for AR promoter. Input indicates input chromatin at a dilution of 1:50; Neg. CT, negative control supernatant. The relative copy number changes to control are shown as $-\text{Log}_2$ values. *$P < .01$ is for CREB1 Ab. *versus* Neg. CT. Error bars, ±2 SEMs.

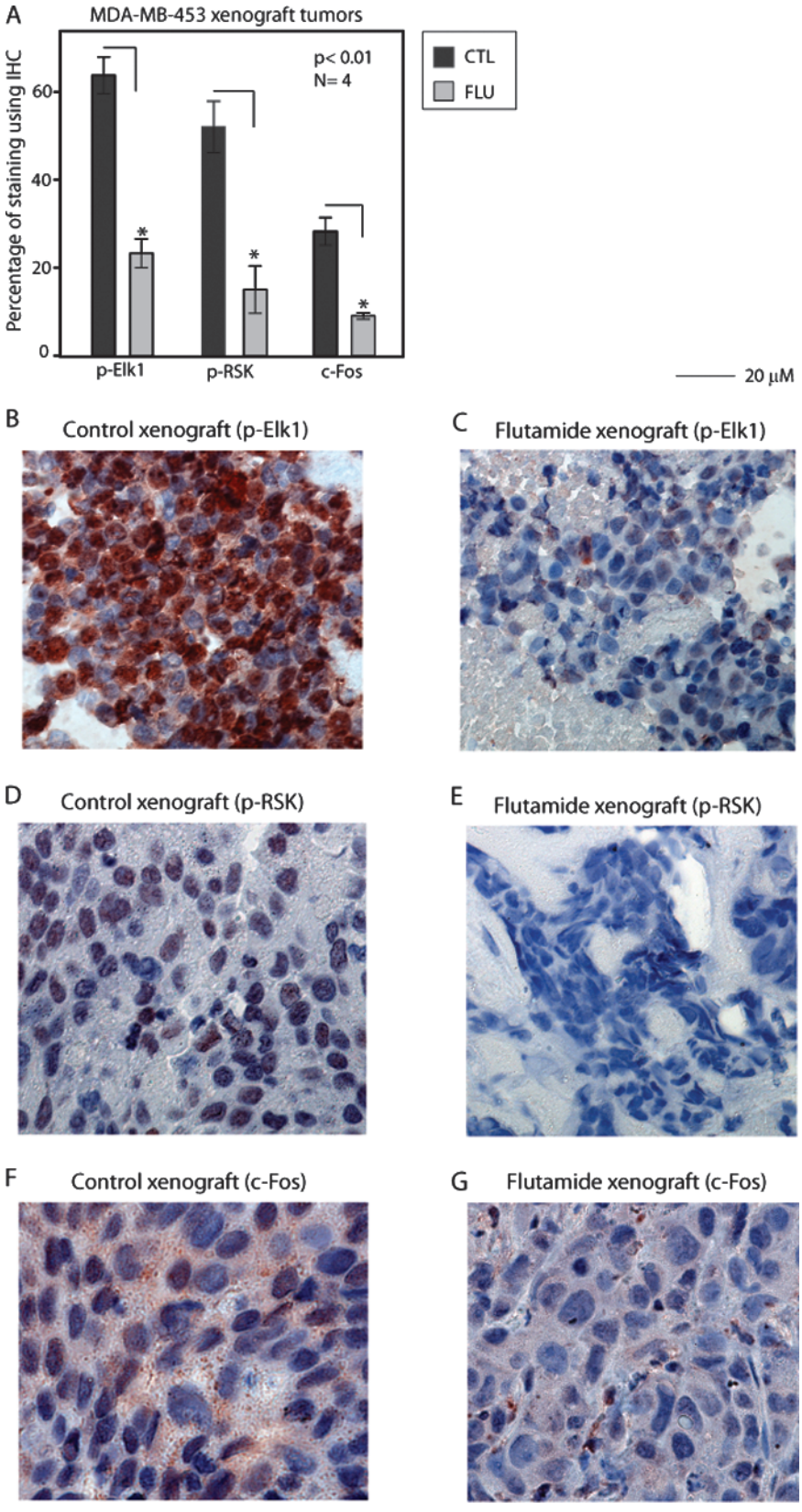

Figure 5. *In vivo* effect of AR inhibition on ERK target proteins. (A) IHC staining for phospho–Elk-1 (p-Elk1), phospho-RSK1 (p-RSK), and c-Fos in xenograft tumors. The percentage of cells positive for each protein was assessed using IHC and compared between flutamide-treated (FLU) and control (CTL) groups. *$P < .01$ is for FLU *versus* CTL. Error bars, ±2 SEMs. (B) Phospho–Elk-1 (p-Elk1) IHC in a control xenograft tumor. Magnification, ×60. (C) Phospho–Elk-1 (p-Elk1) IHC in a flutamide-treated xenograft tumor. Magnification, ×60. (D) Phospho-RSK1 (p-RSK) IHC in a control xenograft tumor. Magnification, ×60. (E) Phospho-RSK1 (p-RSK) IHC in a flutamide-treated xenograft tumor. Magnification, ×60. (F) c-Fos IHC in a control xenograft tumor. Magnification, ×60. (G) c-Fos IHC in a flutamide-treated xenograft tumor. Magnification, ×60.

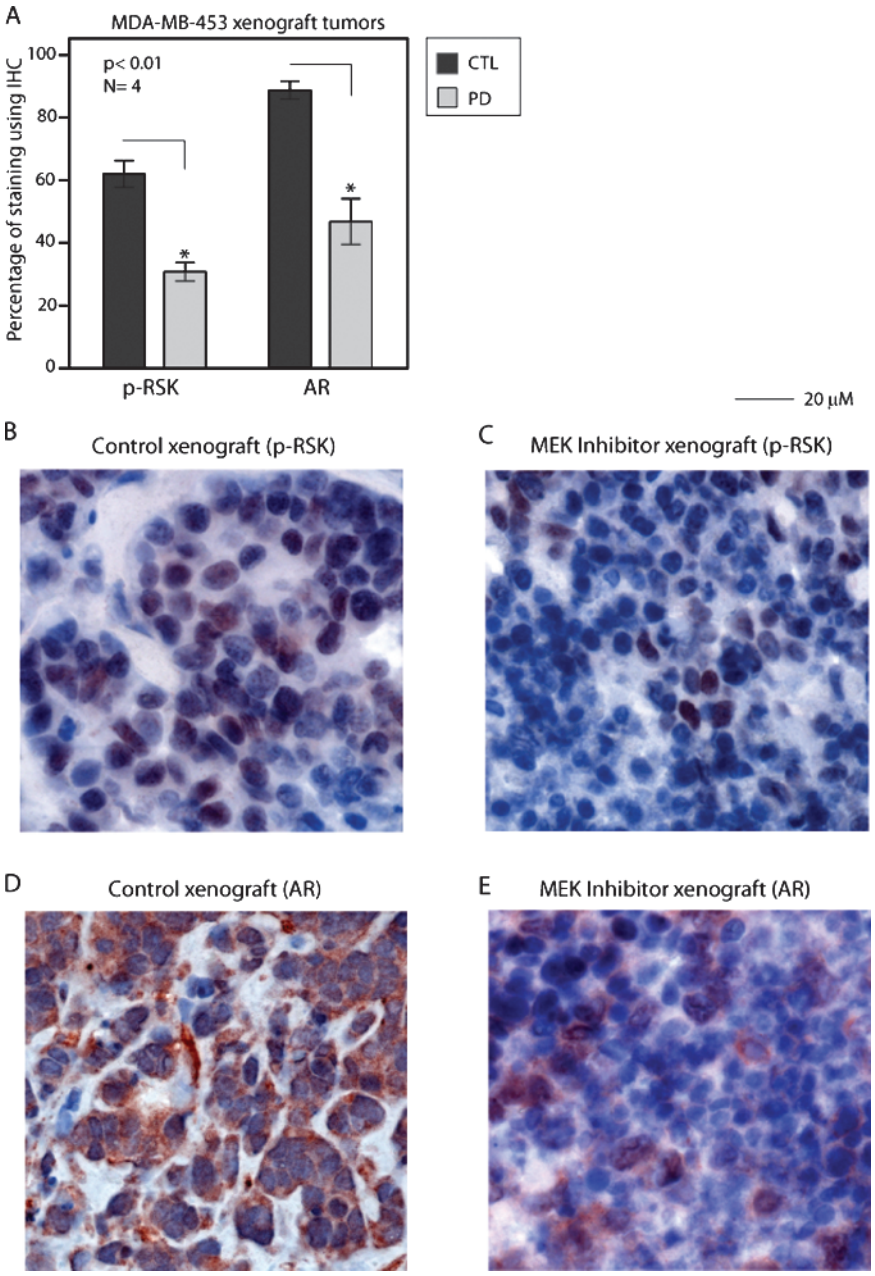

Figure 6. *In vivo* effect of MEK inhibition on AR expression. (A) IHC staining for phospho-RSK1 (p-RSK) and AR in xenograft tumors. The percentage of cells positive for each protein was assessed using IHC and compared between MEK inhibitor–treated (PD) and control (CTL) groups. *$P < .01$ is for PD *versus* CTL. Error bars, ±2 SEMs. (B) Phospho-RSK1 (p-RSK) IHC in a control xenograft tumor. Magnification, ×60. (C) Phospho-RSK1 (p-RSK) IHC in a MEK inhibitor–treated xenograft tumor. Magnification, ×60. (D) AR IHC in a control xenograft tumor. Magnification, ×60. (E) AR IHC in a MEK inhibitor–treated xenograft tumor. Magnification, ×60.

for phospho-RSK1 and AR using IHC. The percentage of cells stained with each antibody was compared between MEK inhibitor and control groups.

We observed an approximately 50% lower phospho-RSK1 staining in the treatment group compared with the controls, suggesting a successful *in vivo* down-regulation of ERK signaling with MEK inhibition ($P < .01$; Figure 6, *A–C*). We next evaluated AR expression in the treatment and control groups. Importantly, the percentage of AR staining was markedly lower in the treated tumors at 45% compared with the controls at 90% ($P < .01$; Figure 6, *A* and *D–E*). These data demonstrate that there is an *in vivo* reduction in AR expression after the inhibition of ERK signaling in molecular apocrine tumors.

AR+/ER– Primary Breast Tumors Have High Expression of phospho–Elk-1 and c-Fos

To further study our *in vitro* and *in vivo* results, we evaluated a cohort of ER– primary breast tumors for a possible association between the expression of AR and ERK target proteins. We first carried out IHC staining for AR in a total of 24 ER– breast tumors and classified these tumors into AR+ and AR– subgroups as described in the Materials and Methods section. A total of 12 samples (50% of tumors) showed AR+ staining in this cohort. We next carried out IHC staining for the ERK target proteins phospho–Elk-1, phospho-RSK1, and c-Fos in these breast tumors and compared the percentage of positive staining for each protein between AR+ and AR– samples.

It is notable that AR+ breast tumors showed a significantly higher expression of phospho–Elk-1 (63% ± 4%) compared with AR– breast tumors (48% ± 5%, $P < .03$; Figure 7, *A–C*). Furthermore, c-Fos expression was significantly higher in AR+ (48% ± 3%) compared with that in AR– samples (34% ± 3%, $P < .03$; Figure 7, *A* and *D–E*). However, the difference between phospho-RSK1 staining did not reach statistical significance (Figure 7*A*). These findings indicate that AR+ staining is associated with a relative overexpression of ERK target proteins phospho–Elk-1 and c-Fos in ER– breast tumors.

Discussion

ER– breast cancer is heterogeneous, and the biology of this disease has remained poorly understood. Study of key signaling pathways mediating the development of ER– breast cancer is a necessary step for the discovery of targeted therapy strategies in this disease. Previous expression microarray studies have identified a distinct molecular apocrine subtype in ER– breast cancer that is characterized by the overexpression of steroid-response genes such as *AR* and a high rate of ErbB2 amplification [2–4]. We have recently demonstrated a functional cross

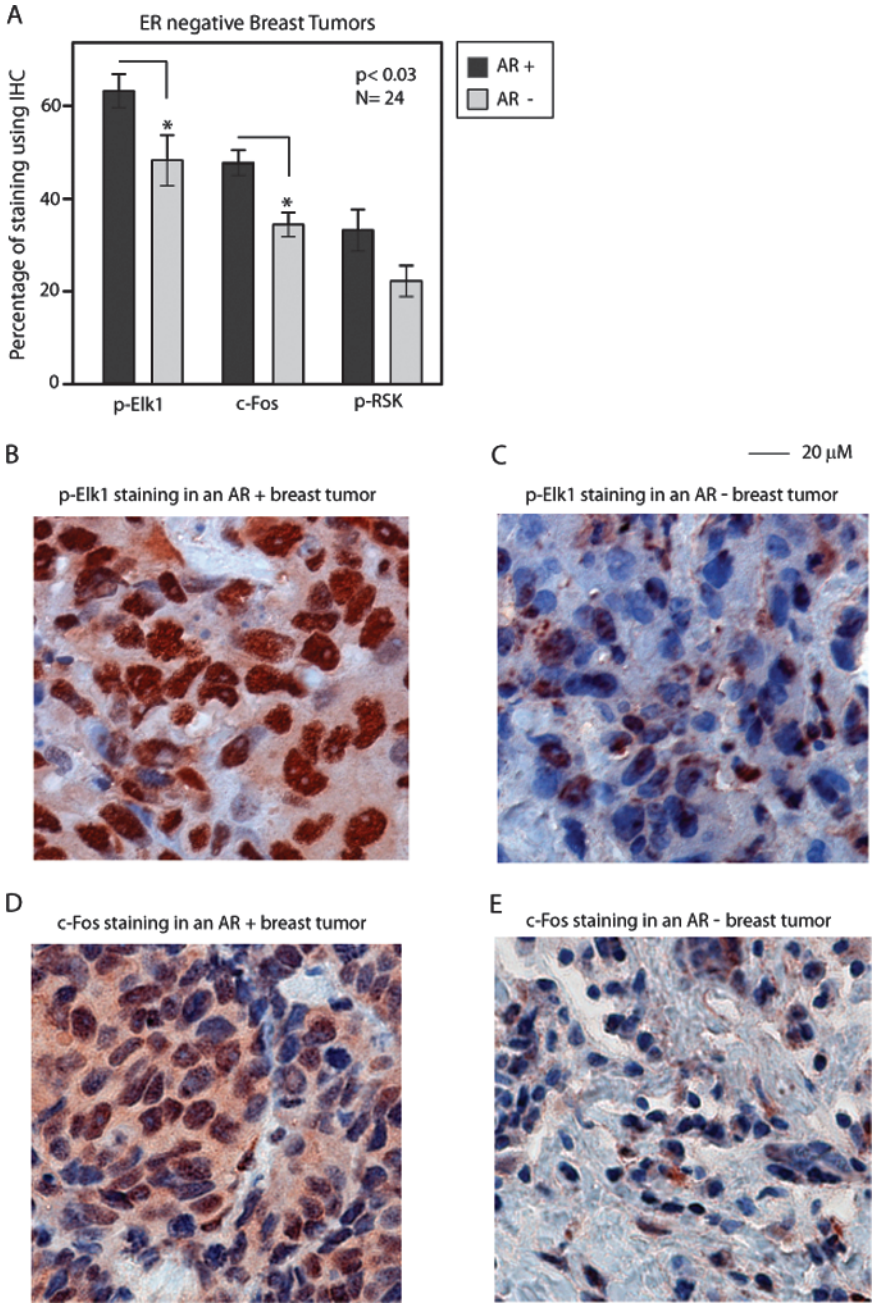

Figure 7. IHC in primary breast tumors. (A) IHC staining for phospho–Elk-1 (p-Elk1), c-Fos, and phospho-RSK1 (p-RSK) in ER-negative (ER−) breast tumors. AR+ group indicates 20% of cells or more showing positive AR staining; AR− group, less than 20% of cells stained for AR. The percentage of cells with positive staining is demonstrated for each group. *$P < .03$ is for AR+ *versus* AR−. Error bars, ±2 SEMs. (B) Phospho–Elk-1 (p-Elk1) IHC in an AR+ breast tumor. Magnification, ×60. (C) Phospho–Elk-1 (p-Elk1) IHC in an AR− breast tumor. Magnification, ×60. (D) c-Fos IHC in an AR+ breast tumor. Magnification, ×60. (E) c-Fos IHC in an AR− breast tumor. Magnification, ×60.

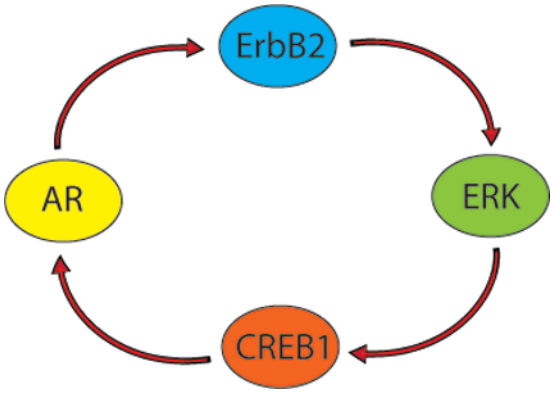

Figure 8. Schematic diagram of an AR-ERK feedback loop involving ErbB2 and CREB1 in molecular apocrine breast cancer. Red arrows depict stimulatory effects.

talk between AR and ErbB2 involving the cross-regulation of steroid-response genes in this subtype [5]. Furthermore, we observed that ERK phosphorylation was modulated in the process of this cross talk [5]. In the present study, we have investigated a feedback loop between AR and ERK signaling in molecular apocrine breast cancer (Figure 8).

One aspect of this feedback loop involves AR regulation of the ERK signaling pathway. This is evident by the fact that AR activity is both necessary and sufficient for the induction of ERK phosphorylation in molecular apocrine cells (Figures 1 and 2). Furthermore, this stimulatory effect of AR is observed at the level of ERK kinase activity. Interestingly, a similar time-dependent AR-mediated induction of ERK has been reported in prostate cancer models [28,29]. In addition, the effect of AR inhibition in reducing ERK phosphorylation is reproducible using different approaches including AR inhibition with flutamide, synergy between flutamide and a low-dose MEK inhibitor, and AR knockdown (Figures 1 and 2). Moreover, AR inhibition results in the down-regulation of ERK signaling targets phospho–Elk-1, phospho-RSK1, and c-Fos using an *in vivo* xenograft model of molecular apocrine tumors (Figure 5). Taken together, these findings suggest that AR is a regulator of ERK signaling in molecular apocrine cells (Figure 8).

Our data suggest some variation in sensitivity to the effect of AR inhibition/down-regulation on ERK phosphorylation across molecular apocrine cell lines. In this respect, MDA-MB-453 cells are more sensitive to the effect of AR inhibition/down-regulation compared with HCC-1954 cells, and this corresponds to a higher level of AR expression in MDA-MB-453 line (Figures 1 and 2). It is notable that the level of ER expression has been associated with a better response to anti-estrogen therapy in ER+ breast cancer [30,31]. Future clinical studies are required to determine whether variation in AR expression levels can similarly act as a predictive marker for sensitivity to AR inhibition in molecular apocrine patients.

ErbB2 is a known activator of ERK signaling, and it induces AR transactivation through the ERK pathway in prostate cancer [22,32,33]. Furthermore, there is a cross talk between AR and ErbB2 at the functional and genomics levels in molecular apocrine breast cancer [5,11]. Here, we have demonstrated that AR-mediated induction of ERK requires ErbB2. In turn, AR activity is necessary and sufficient for ErbB2 expression and ErbB2 is an AR target gene (Figure 3). These findings are supported by our previous report that androgens induce ErbB2 mRNA expression in molecular apocrine cells [5]. Therefore, the transcriptional regulation of ErbB2 by AR provides a molecular mechanism for AR modulation of the ERK signaling pathway. Although there may be additional mechanisms contributing to the interaction between AR and ERK, our data suggest that ErbB2 is a key component of this feedback loop and an upstream connector between the AR and ERK signaling pathways (Figure 8). Moreover, a functionally active AR signaling may contribute to the high prevalence of ErbB2 overexpression in molecular apocrine cells, which, in turn, can lead to the activation of ERK signaling in this subtype of breast cancer.

Another aspect of the AR-ERK feedback loop is an ERK-mediated regulation of AR expression in molecular apocrine cells (Figure 8). In this process, inhibition of ERK phosphorylation results in the down-regulation of AR expression using both *in vitro* and *in vivo* models of molecular apocrine breast cancer (Figures 4 and 6). Interestingly, regulation of AR activity by the ERK signaling pathway has also been observed in prostate cancer models and may contribute to the progression of this disease [15,34]. Furthermore, our data suggesting that AR is a CREB1 target gene provides a mechanism for the observed ERK-mediated regulation of AR in molecular apocrine cells (Figure 4). CREB1 is a well-characterized ERK signaling transcription factor and, as a part of the MEK1/2-ERK1/2-CREB1 pathway, is a mediator of androgen signaling in prostate cancer [23–25,29]. In this respect, CREB1 is a downstream target of active ERK through the mediation of RSK and MSK family of kinases, which, on activation, stimulates transcription of a variety of genes [24,25,35–37]. Therefore, CREB1-mediated regulation of AR transcription would act as a downstream connector between the AR and ERK signaling pathways (Figure 8).

Our findings in ER– breast tumors for an association between AR-positive staining and overexpression of ERK signaling targets phospho–Elk-1 and c-Fos further supports a cross-regulation between the AR and ERK signaling pathways in molecular apocrine breast cancer (Figure 7). It is notable that c-Fos is also a CREB1 target gene and is regulated in an androgen-dependent way in prostate cancer models [25,29]. Therefore, in addition to overexpression of steroid-response genes [3], there is a relative overexpression of ERK signaling targets in molecular apocrine breast tumors.

In summary, we have identified a positive feedback loop between the AR and ERK signaling pathways in molecular apocrine breast cancer. In this feedback loop, AR regulates ERK phosphorylation through the mediation of ErbB2 and, in turn, ERK-CREB1 signaling regulates the transcription of AR in molecular apocrine cells. The biologic significance and a potential for targeted therapy highlight the importance of this feedback loop in ER– breast cancer.

Acknowledgments

The authors thank Kim Woolley from The University of Queensland Biological Research Facility for assistance with animal work.

References

[1] Putti TC, El-Rehim DM, Rakha EA, Paish CE, Lee AH, Pinder SE, and Ellis IO (2005). Estrogen receptor–negative breast carcinomas: a review of morphology and immunophenotypical analysis. *Mod Pathol* **18**, 26–35.

[2] Farmer P, Bonnefoi H, Becette V, Tubiana-Hulin M, Fumoleau P, Larsimont D, Macgrogan G, Bergh J, Cameron D, Goldstein D, et al. (2005). Identification of molecular apocrine breast tumours by microarray analysis. *Oncogene* **24**, 4660–4671.

[3] Teschendorff AE, Naderi A, Barbosa-Morais NL, and Caldas C (2006). PACK: Profile Analysis using Clustering and Kurtosis to find molecular classifiers in cancer. *Bioinformatics* **15**, 2269–2275.

[4] Doane AS, Danso M, Lal P, Donaton M, Zhang L, Hudis C, and Gerald WL (2006). An estrogen receptor–negative breast cancer subset characterized by a

hormonally regulated transcriptional program and response to androgen. *Oncogene* **25**, 3994–4008.

[5] Naderi A and Hughes-Davies L (2008). A functionally significant cross-talk between androgen receptor and ErbB2 pathways in estrogen receptor negative breast cancer. *Neoplasia* **10**, 542–548.

[6] Niemeier LA, Dabbas DJ, Beriwal S, Striebel JM, and Bhargava R (2009). Androgen receptor in breast cancer: expression in estrogen receptor–positive tumors and in estrogen receptor–negative tumors with apocrine differentiation. *Mod Pathol* **23**, 205–212.

[7] Park S, Koo J, Park HS, Kim JH, Choi SY, Lee JH, Park BW, and Lee KS (2009). Expression of androgen receptors in primary breast cancer. *Ann Oncol* **21**, 488–492.

[8] Vranic S, Tawfik O, Palazzo J, Bilalovic N, Eyzaguirre E, Lee LMJ, Adegboyega P, Hagenkord J, and Gatalica Z (2010). EGFR and HER-2/*neu* expression in invasive apocrine carcinoma of the breast. *Mod Pathol* **23**, 644–653.

[9] Banneau G, Guedj M, Macgrogan G, de Mascarel L, Velasco V, Schiappa R, Bonadona V, David A, Dugast C, Gilbert-Dussardier B, et al. (2010). Molecular apocrine differentiation is a common feature of breast cancer in patients with germline PTEN mutations. *Breast Cancer Res* **12**, R63.

[10] Naderi A and Liu J (2010). Inhibition of androgen receptor and Cdc25A phosphatase as a combination targeted therapy in molecular apocrine breast cancer. *Cancer Lett* **298**, 74–87.

[11] Sanga S, Broom BM, Cristini V, and Edgerton ME (2009). Gene expression meta-analysis supports existence of molecular apocrine breast cancer with a role for androgen receptor and implies interactions with ErbB family. *BMC Med Genomics* **2**, 59.

[12] Frodin M and Gammeltoft S (1999). Role and regulation of 90 kDa ribosomal S6 kinase (RSK) in signal transduction. *Mol Cell Endorcinol* **151**, 65–77.

[13] Cruzalegui FH, Cano E, and Treisman R (1999). ERK activation induces phosphorylation of Elk-1 at multiple S/T-P motifs to high stoichiometry. *Oncogene* **18**, 7948–7957.

[14] Yarden Y and Sliwkowski MX (2001). Untangling the ErbB signalling network. *Nat Rev Mol Cell Biol* **2**, 127–137.

[15] Shigemura K, Isotani S, Wang R, Fujisawa M, Gotoh A, Marshall FF, Zhau HE, and Chung LW (2009). Soluble factors derived from stroma activated androgen receptor phosphorylation in human prostate LNCaP cells: roles of ERK/MAP kinase. *Prostate* **69**, 949–955.

[16] Leotoing L, Manin M, Monte D, Baron S, Communal Y, Lours C, Veyssiere G, Morel L, and Beaudoin C (2007). Crosstalk between androgen receptor and epidermal growth factor receptor–signalling pathways: a molecular switch for epithelial cell differentiation. *J Mol Endocrinol* **39**, 151–162.

[17] Naderi A, Liu J, and Bennett IC (2010). BEX2 regulates mitochondrial apoptosis and G_1 cell cycle in breast cancer. *Int J Cancer* **126**, 1596–1610.

[18] Naderi A, Teschendorff AE, Beigel M, Cariati M, Ellis IO, Brenton JD, and Caldas C (2007). BEX2 is overexpressed in a subset of primary breast cancers and mediates nerve growth factor/nuclear factor-kappaB inhibition of apoptosis in breast cancer cell lines. *Cancer Res* **67**, 6725–6736.

[19] Naderi A, Liu J, and Hughes-Davies L (2010). BEX2 has a functional interplay with c-Jun/JNK and p65/RelA in breast cancer. *Mol Cancer* **19**, 111.

[20] Cariati M, Naderi A, Brown JP, Smalley MJ, Pinder SE, Caldas C, and Purushotham AD (2008). α_6 Integrin is necessary for the tumourigenicity of a stem cell–like sub-population within the MCF7 breast cancer cell line. *Int J Cancer* **122**, 298–304.

[21] Hoeflich KP, O'Brien C, Boyd Z, Cavet G, Guerrero S, Jung K, Januario T, Savage H, Punnoose E, Truong T, et al. (2009). *In vivo* antitumor activity of MEK and phosphatidylinositol 3-kinase inhibitors in basal-like breast cancer models. *Clin Cancer Res* **15**, 4649–4664.

[22] Bourguignon LY, Gilad E, and Peyrollier K (2007). Heregulin-mediated ErbB2-ERK signaling activates hyaluronan synthases leading to CD44-dependent ovarian tumor cell growth and migration. *J Biol Chem* **282**, 19426–19441.

[23] Lonze BE and Ginty DD (2002). Function and regulation of CREB family transcription factors in the nervous system. *Neuron* **35**, 605–623.

[24] Xing J, Ginty D, and Greenberg ME (1996). Coupling of the RAS-MAPK pathway to gene activation by RSK2, a growth factor–regulated CREB kinase. *Science* **273**, 959–963.

[25] De Cesare D, Jacquot S, Hanauer A, and Sassone-Corsi P (1998). Rsk-2 activity is necessary for epidermal growth factor–induced phosphorylation of CREB protein and transcription of c-*fos* gene. *Proc Natl Acad Sci USA* **95**, 12202–12207.

[26] Yang SH, Yates PR, Whitmarsh AJ, Davis RJ, and Sharrocks AD (1998). The Elk-1 ETS-domain transcription factor contains a mitogen-activated protein kinase targeting motif. *Mol Cell Biol* **18**, 710–720.

[27] Wang Y and Prywes R (2000). Activation of the c-*fos* enhancer by the Erk MAP kinase pathway through two sequence elements: the c-*fos* AP-1 and p62TCF sites. *Oncogene* **19**, 1379–1385.

[28] Peterziel H, Mink S, Schonert A, Becker M, Klocker H, and Cato AC (1999). Rapid signalling by androgen receptor in prostate cancer cells. *Oncogene* **18**, 6322–6329.

[29] Unni E, Sun S, Nan B, McPhaul MJ, Cheskis B, Mancini MA, and Marcelli M (2004). Changes in androgen receptor nongenotropic signaling correlate with transition of LNCaP cells to androgen independence. *Cancer Res* **64**, 7156–7168.

[30] Diaz LK and Sneige N (2005). Estrogen receptor analysis for breast cancer: current issues and keys to increasing testing accuracy. *Adv Anat Pathol* **12**, 101–109.

[31] Harvey LM, Clark GM, Osborne CK, and Allred DC (1999). Estrogen receptor status by immunohistochemistry is superior to the ligand-binding assay for predicting response to adjuvant endocrine therapy in breast cancer. *J Clin Oncol* **17**, 1474–1481.

[32] Yeh S, Lin HK, Kang HY, Thin TH, Lin MF, and Chang C (1999). From HER2/Neu signal cascade to androgen receptor and its coactivators: a novel pathway by induction of androgen target genes through MAP kinase in prostate cancer cells. *Proc Natl Acad Sci USA* **96**, 5458–5463.

[33] Craft N, Shostak Y, Carey M, and Sawyers CL (1999). A mechanism for hormone-independent prostate cancer through modulation of androgen receptor signaling by the HER-2/*neu* tyrosine kinase. *Nat Med* **5**, 280–285.

[34] Carey AM, Pramanik R, Nicholson LJ, Dew TK, Martin FL, Muir GH, and Morris JDH (2007). Ras-MEK-ERK signaling cascade regulates androgen receptor element–inducible gene transcription and DNA synthesis in prostate cancer cells. *Int J Cancer* **121**, 520–527.

[35] Xing J, Kornhauser JM, Xia Z, Thiele EA, and Greenberg ME (1998). Nerve growth factor activates extracellular signal–regulated kinase and p38 mitogen-activated protein kinase pathways to stimulate CREB serine 133 phosphorylation. *Mol Biol Cell* **18**, 1946–1955.

[36] Wiggin GR, Soloaga A, Foster JM, Murray-Tait V, Cohen P, and Arthur JS (2002). MSK1 and MSK2 are required for the mitogen- and stress-induced phosphorylation of CREB and ATF1 in fibroblasts. *Mol Biol Cell* **22**, 2871–2881.

[37] Mayr B and Montminy M (2001). Transcriptional regulation by the phosphorylation-dependent factor CREB. *Nat Rev Mol Cell Biol* **2**, 599–609.